Colloidal Systems with Attractive Interactions: Evaluation of Scattering Data Using the Generalized Indirect Fourier Transformation Method

Josef Innerlohinger,[†] Hans M. Wyss,[‡] and Otto Glatter*,[†]

Physical Chemistry, Institute of Chemistry, Karl-Franzens University, 8010 Graz, Austria, and Nonmetallic Materials, Department of Materials, ETH Zurich, 8092 Zurich, Switzerland

Received: July 19, 2004; In Final Form: August 30, 2004

Different attractive interacting colloidal systems are characterized by means of static light scattering. As most of these samples are rather concentrated, multiple scattering is suppressed by partial contrast match and the use of very a thin sample cell (13 μm). This is possible with the laboratory built flat cell light scattering instrument, which is also capable of time-resolved measurements. The systems under investigation are oil-in-water emulsions with added polymer micelles or latex spheres, which give rise to depletion interaction. A second set of samples consists of electrostatically stabilized dense silica suspensions, which are destabilized by ionic strength or pH shift initiated by an in-situ reaction. The potential change from repulsive to attractive is measured time-resolved in real time. These suspensions are model systems for the so-called direct coagulation casting (DCC) method. Scattering data are evaluated using the generalized indirect Fourier transformation (GIFT) method. We added some new routines for calculating structure factors for attractively interacting systems to the already existing software package. We now can choose between a depletion interaction and an attractive square well potential, which was used for the DCC samples. The obtained results are in good agreement with the values known from preparation for the depletion samples and those predicted from DLVO calculations for the DCC series, respectively.

1. Introduction

Colloidal science is a rather broad field, which covers a lot of different topics ranging from physics over chemistry to biology.[1−4] Over the past few few years especially the attractive interaction in colloidal systems has become the subject of an ever increasing number of studies.[5−9] To understand and control these interactions is of both basic scientific interest and importance for applications.

Scattering methods[10] are a well established tool in studying colloidal systems. The evaluation of scattering data from attractively interacting systems is still a challenging problem. In the presented work we use the generalized indirect Fourier transformation (GIFT) technique for the evaluation of static light scattering data from various attractively interacting systems. The GIFT method allows the simultaneous determination of the particle form factor and the structure factor from the measured scattering intensities. Here we introduce new routines for attractive structure factors to the already existing GIFT software. In this way, we are able to evaluate the scattering data and obtain good results with minimum a priori information. The measurement itself is also not a trivial task, because we examine turbid concentrated samples. We avoid multiple scattering by using very thin sample cells and partial contrast match.

We investigate two different types of systems in this study. First, we study a model system for the *direct coagulation casting process* (DCC), a novel method for the production of high performance ceramics. This system consists of electrostatically stabilized silica spheres in aqueous suspension. Aggregation is induced by continuously decreasing the electrostatic repulsion via an internal chemical reaction. Second, we study systems with attractive depletion interaction. We use o/w (oil/water) emulsions with added surfactant micelles or latex spheres for this part of our study. The model system is tuned to match our experimental and evaluation window, and thus allowing us to obtain useful results.

The possibilities and limitations of evaluating light scattering data from attractively interacting systems are discussed.

2. Theory

2.1. Static Light Scattering. In static light scattering the time-averaged mean intensity of light, scattered by particles in solution, is measured as a function of the scattering angle θ. Measuring time is several seconds up to minutes. The scattering angle is related to the magnitude of the scattering vector q by

$$q = \frac{4\pi n_s'}{\lambda_0} \sin\left(\frac{\theta}{2}\right) \tag{1}$$

n_s' is the real part of the refractive index of the solvent, and λ_0 is the wavelength of the incident beam in a vacuum.

Usually the particles measured in static light scattering are in the same size regime as the used light (several 100 nm). The scattering process for spheres is described by the Lorenz−Mie (LM) theory.[11,12] The scattering intensity of polydisperse systems can be regarded as a linear combination of LM form factors $P(q,R,m)$, where R is the particle radius and m is the complex refractive index ratio of the particles and of the solvent. Because of the low absorption of the particles used, the

* Corresponding author. Institute of Chemistry, Heinrichstrasse 28, 8010 Graz, Austria. Telephone: +43 316 380 5433. E-mail: otto.glatter@uni-graz.at.

[†] Karl-Franzens University.

[‡] ETH Zurich.

10.1021/jp0468105 CCC: $27.50
Published on Web 11/03/2004

imaginary parts of the refractive indices can be neglected. So, m can be approximated by m'.

$$m \cong m' = \frac{n_p'}{n_s'} \tag{2}$$

n_p' is the real part of the refractive index of the particles in solution. The total scattering intensity of a polydisperse system of spheres can be written as

$$I(q) = \int_{R_{min}}^{R_{max}} D(R)P(q,R,m')\, dR \tag{3}$$

$D(R)$ is a continuous function of the intensity weighted contribution of the population, in the range R and $R + dR$.

The simpler Rayleigh−Debye−Gans (RDG) theory[13−15] can be used, if the RDG limit

$$2\alpha(m' - 1) \ll 1 \tag{4}$$

is fulfilled. Here the size parameter α is defined as

$$\alpha = \frac{2\pi R}{\lambda} \tag{5}$$

One can easily see, that condition 4 is not fulfilled for light scattering from particles of a size comparable to the wavelength of light. However, the value of m' can be reduced by contrast variation, i.e., a partial contrast match. So it is possible to shift the scattering from the LM to the RDG regime.

The decrease of the difference between n_p and n_s by varying the latter also reduces the scattering power of the particles and so multiple scattering. This is another benefit of contrast variation, as the contribution of multiple scattering to the total scattered intensity can already be essential at moderate concentrations. At higher concentrations the contribution of multiple scattering interferes with that of the particle interactions, that we are interested in. Thus, an evaluation of this scattering data with respect to the particle interactions would not be possible even in the RDG regime. Partial contrast match (m' close to 1) is, however, in many cases not enough for a reduction of multiple scattering to a negligible amount. This can finally be achieved by using extremely thin sample cells.

2.2. Generalized Indirect Fourier Transformation. In the RDG regime the total scattering intensity $I(q)$ for homogeneous monodisperse spherical particles can be expressed as the following product[16]

$$I(q) = nP(q)S(q) \tag{6}$$

where n is the particle density (N/V), $P(q)$ is the ensemble averaged form factor, and $S(q)$ is the structure factor. $S(q)$ gives information about the spatial arrangement of the particles. Factorization according to eq 6 is also possible for polydisperse spherical particles. In this case $S(q)$ represents an *effective* or *measured* structure factor.[16,17] This approach can also be formally extended to nonspherical systems. $P(q)$ contains the information about the size and shape of the particles and can be Fourier transformed into the pair distance distribution function $p(r)$.

A simultaneous determination of the form factor $P(q)$ and the structure factor $S(q)$ from scattering curves in the RGD limit is possible with the GIFT method.[17,18] The form factor is calculated model free by using the indirect Fourier transformation technique.[19] Here only a rough estimate for the maximum particle dimension D_{max} has to be given. Different closure relations like Percus−Yevick (PY),[20] Rogers−Young (RY)[21] or HMSA[22] and interaction potentials like hard sphere, square well, or depletion potential can be chosen for the evaluation of the structure factor. A Boltzmann simplex simulated annealing (BSSA)[23] algorithm is used to search for the structure factor, which fits best to the measured data. To keep the values for the parameters defining $S(q)$ within a physically reasonable regime, limits for these values for the BSSA search have to be set by the user.

As already mentioned above, multiple scattering can bias the interesting information contained in a scattering curve and can make an evaluation impossible. In a previous paper[24] it was shown that a transmission higher than 0.7 is needed in order to obtain correct solutions with GIFT.

2.3. Depletion Interaction. The effective sphere−sphere interaction potential U_{dep} for hard spheres in the presence of nonadsorbing polymers, derived by Asakura and Oosawa[25,26] and Vrij,[27] is given by

$$U_{dep} = \begin{cases} +\infty & \text{for } r \le \sigma \\ -\Pi_p V_{overlap} & \text{for } \sigma < r \le \sigma + 2r_g \\ 0 & \text{for } r > \sigma + 2r_g \end{cases} \tag{7}$$

where r is the center-center distance between the spheres with diameter σ. Π_p is the osmotic pressure of the polymer solution in equilibrium with the mixture, r_g is the gyration radius of the polymers and $V_{overlap}$ the volume of the overlapping depletion zones of two spheres at center-center distance r. These depletion zones are the region around each colloidal particle, which is not accessible to the center of the polymers, so it has a thickness on the order of r_g. If now the depletion regions of two particles overlap, there is an unbalanced osmotic pressure pushing the particles together, which can be expressed by the attractive potential U_{dep} given above.

One of the simplifications introduced by Asakura and Oosawa was to treat the polymer coils as hard spheres with a radius r_g. The above potential therefore is also valid for big particles in the presence of small particles, which both act as hard spheres; r_g in the equations than represents the radius of the smaller particles.

The range of this potential is clearly given by the size of the small particles. The depth again is related to size of the small particles or more precisely to the size ratio, which is contained in $V_{overlap}$, but mainly determined by the concentration of the small particles. For an ideal solution the osmotic pressure is given by

$$\Pi_p = n_p^{(R)} k_B T \tag{8}$$

The number density $n_p^{(R)}$ is the number of small particles in the volume accessible to them, the so-called free volume.[28] This means that the volume of the big particles and their depletion zones must be subtracted from the total volume giving the free volume. So the actual number density of the small particles is $n_p = \alpha n_p^{(R)}$, with α being the free volume fraction. It can be approximated as[29]

$$\alpha = (1 - \phi) \exp(-A\gamma - B\gamma^2 - C\gamma^3) \tag{9}$$

where ϕ is the volume fraction of the big particles, $\gamma = \phi/(1 - \phi)$, $A = 3\xi + 3\xi^2 + \xi^3$, $B = 9\xi/2 + 3\xi^3$, and $C = \xi^3$. Here ξ is the already mentioned size ratio between small and big particles, given by

$$\xi = \frac{2r_g}{\sigma} \tag{10}$$

For $\xi < 0.1$ the following rather good approximation[30] can be used for the depletion potential in the range $\sigma < r < \sigma + 2r_g$

$$u(r) = -\eta_p^{(R)} k_B T \frac{3}{2} \frac{1+\xi}{\xi^3} \left(\frac{r}{\sigma} - 1 - \xi\right)^2 \qquad (11)$$

where $\eta_p^{(R)}$ is the volume fraction of the small particles in the free volume.

3. Materials and Methods

3.1. Silicone Oil Emulsions. The silicone oil emulsions for this study are o/w emulsions consisting of silicone oil DC200 (Fluka), the nonionic surfactant Triton X100 (Sigma Aldrich), and deionized water (Milli-Q RG). The emulsions are obtained by shearing a crude hand-mixed emulsion (50−60 wt % silicone oil and a 33 wt % Triton X100 solution) in a laboratory-built shear apparatus.[24] This shear apparatus is based on the idea of a Couette cell.[31] The width of the size distribution of the emulsion is further reduced by the fractionated crystallization technique.[32] In this step the excess of surfactant is also removed from the system by repeatedly washing with distilled water and centrifugation. This is important, because later surfactant micelles are added in a controlled manner to trigger depletion interaction.

We prepared two different emulsions with a medium droplet radius of 570 nm respectively 400 nm and oil concentrations around 45 wt %. The remaining Triton X100 content is below 1 wt % and shows no significant influence.

3.2. Silica Suspensions and Direct Coagulation Casting. Monospher 500 (Merck) silica particles, which have a very narrow size distribution and spherical shape (average diameter: 525 nm), are used for the production of the suspensions. A second batch of this silica was coated with Boehmite. Suspensions containing uncoated or coated silica are prepared according to the procedure described in a previous paper.[33] These suspensions are used to study change of the potential during the DCC process.[34,35] This is a recently developed method, which allows an in situ homogeneous destabilization of highly concentrated suspensions via an internal enzyme catalyzed reaction. In our case, we use the hydrolysis of urea catalyzed by the enzyme urease. This reaction can either cause a pH shift toward pH = 9 (buffer region of this reaction) or, starting at pH = 9, increase the ionic strength in the solution. In the following, we will refer to the two different mechanisms and systems as the ΔpH method and the Δ*I* method, respectively. Making use of the different isoelectric points (IEP) of uncoated and coated silica, both mechanisms can be used for the DCC process.

For the ΔpH method, we use a 30 vol % suspension of coated silica (IEP at pH = 9) in an aqueous phase containing 30 wt % sucrose for partial index match and 10 wt % urea. This system is electrostatically stabilized at pH = 4. We add 5 units/mL urease to the cooled suspension. At room temperature, the hydrolysis reaction speeds up and shifts the pH toward 9, where the surface charge of the silica is neutralized and it is no longer stabilized.

For the Δ*I* method, we use uncoated silica (30 vol % in 40 wt % sucrose, 6.4 wt % urea). This system is electrostatically stabilized at pH = 9 with the silica having the IEP at pH = 3. To induce the hydrolysis reaction, 50units/mL urease are added, leading to a continuous increase of ionic concentration in the liquid phase. The salt produced screens the electrostatic repulsion between the silica and the system starts to aggregate.

The different composition of the samples for the destabilizations results from the circumstances of the chosen method. For the Δ*I* method, less urea, which also increases n_s', is needed. Therefore, we have to add more sucrose to this sample to achieve the desired partial contrast match. The enzyme activity is chosen in a way that the destabilization can be followed in real-time with our instrument.

3.3. Depletion Interaction. To induce depletion interaction a defined excess of Triton X100 is added to the silicone oil emulsions. This is done by mixing a highly concentrated emulsion with an aqueous Triton X100 solution. The spherical Triton X100 micelles lead to an attractive depletion potential between the emulsion droplets. Alternatively aqueous suspensions of latex spheres are added to the emulsions. In this case we use polystyrene latices (IDC, Portland, Oregon) with diameters of 26 nm (±18%) and 76 nm (±7%). Both the Triton X100 solution and the latex suspension are added very carefully and slowly to the emulsion to prevent coalescence. The approximate compositions of the samples after preparation are as follows:

(1) 30 vol % emulsion A (R = 570 nm) + 4 vol % Triton X100 in 30 wt % sucrose aqueous solution.

(2) 18 vol % emulsion A + 4 vol % latex (26 nm or 76 nm) in 30 wt % sucrose aqueous solution.

(3) 20 vol % emulsion B (R = 400 nm) + 7 vol % Triton X100 in 30 wt % sucrose aqueous solution.

(4) 20 vol % emulsion B + 3 vol % latex (26 nm) in 23 wt % sucrose aqueous solution.

The Triton X100 concentration in these samples is above the cmc (~1.3 vol %).

Similarly, we added a suspension of 26 nm latex to a pure suspension of uncoated silica (not containing urea or urease) to study depletion interaction with solid colloids. The composition of this sample is 8.5 vol % silica and 5 vol % 26 nm latex in a 45 wt % sucrose aqueous solution.

3.4. Contrast Variation. Sucrose extra pure (Merck) is used to reduce the refractive index ratios m of the suspensions/emulsions. Again sucrose is added very carefully and slowly to the oil emulsions. This is to prevent breaking of the droplets due to the osmotic pressure resulting from very different sucrose concentrations. For these experiments we used sucrose concentrations between 23 and 45 wt % related to the aqueous phase, which results in refractive indices n_s' between 1.368 and 1.410. The other used components have the following refractive indices: silicone oil $n_p' = 1.405$, silica $n_p' = 1.417$, and latex $n_p' = 1.591$.

3.5. Static Light Scattering Setup. We use a laboratory built flat cell light scattering instrument (FCLSI)[36] for the measurements. This instrument simultaneously detects the scattering curve from 1 to 60° (maximum) via diode arrays consisting of 160 photodiodes. As light source a 10 mW HeNe laser with random polarization and a wavelength of 632.8 nm is used. The diode array allows the achievement of short measurement times. By default, 10 curves with a measurement time of 20 s each are recorded and averaged automatically. For the destabilization experiments, we measure single curves with a duration of 20 s. This allows us to follow change of the potential in real time. Here, 20 s/curve is a good compromise between measuring speed and data quality.

The sample cell has two parallel optical flats, which can be adjusted at various fixed distances. The smallest achievable cell thickness is 13 μm. We use this thickness for the destabilization studies. For the other samples, we typically use a cell thickness of 25 μm. The thin sample cell and contrast variation with sucrose reduce multiple scattering to a negligible amount and

allow the measurement of dense turbid systems. The increase of the refractive index of the aqueous phase lowers the m' value and thus allows the application of the RDG theory. This is needed for data evaluation using GIFT.

As we combine a thin sample cell with contrast variation, the transmission of the measured samples is always higher than 0.8. Prior to the data evaluation, we subtract the background scattering curve (as measured in a cell filled with sucrose solution), and we convert the data to q-scale.

Beside the advantage of allowing the measurement of turbid systems, the thin sample cell has also a disadvantage, as it can give rise to wall effects, which are discussed in detail in section 4.2.

3.6. Data Evaluation. To determine if the emulsions/suspensions have a narrow monomodal size distribution, scattering curves from very dilute samples were evaluated using the optimized regularization technique (ORT).[37] It calculates size distributions from scattering curves assuming a spherical shape of the particles. For this study we calculate the intensity weighted distribution from which we also get the average radius of our particles.

The scattering curves from the concentrated systems are evaluated applying the GIFT method. We added some new structure factor models for attractive interaction into the existing software package. We now can choose between a simple square well in combination with PY, SMSA, or HMSA closure relation and a depletion potential combined with PY or SMSA closure relation.

We implemented a subroutine[30,38,39] for these potentials and closure relations and adapted it to the needs of our existing software package and to the problems under investigation. The major change is that the original routine scales everything to a colloid diameter σ of 1.0 and one has to enter a certain value dr for the discrete grid spacing in real space. First we altered the routine so that it calculates dr automatically from the q-regime covered by the experiment and the size of the particles. This causes a problem for very narrow widths of the potentials relative to the particle size, because it can happen, that the width of the square well or of the depletion potential is only sampled by one or two points. This leads to wrong structure factors. So an additional check is added that ensures a minimum number of points (at least 5), which sample the potential.

The sub-routine implemented in the GIFT package calculates the depletion potential according to eq 11. The required input parameters therefore are the size ratio between the particles ξ, the volume fraction of the large particles and the volume fraction of the smaller particles in the free volume $\eta_p^{(R)}$. The volume fraction in the free volume needs a little additional attention. Because the value accessible from the experiment (preparation) is usually the volume fraction in the total volume. The difference between these two values can be rather big. Using eq 9 these two values can be easily converted into each other. So one just has to be careful not to mix them up, which could cause misleading results.

The structure factors for both square well and depletion potential are defined by the colloid volume fraction and the interaction radius between the colloids. In the case of the square well, the potential is directly given by the relative well width and the well depth in units of kT. The depletion potential is calculated from the size ratio between the small and large particles and the concentration of the small particles. Both structure factors are thus defined by four parameters, for which reasonable limits have to be set by the user. These four parameters are quasi-linearly dependent, which makes a completely free variation of all four impossible. Usually a priori information is available for one or two parameters allowing us to confine these parameters. Without this confinement it would be possible to get a good fit to the data, but the corresponding parameters could be physically meaningless.

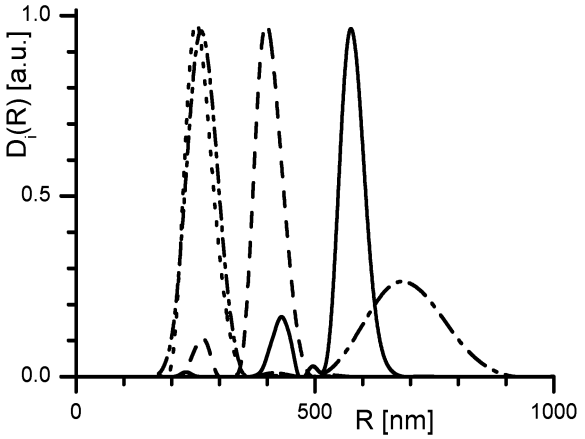

Figure 1. Intensity weighted size distributions for the samples used in this study obtained from scattering curves of diluted systems. For better comparability the main population of each sample has been normalized to one. Solid: emulsion A. Dash: emulsion B. Dot: uncoated silica. Dash−dot: coated silica.

For the evaluation of scattering curves from the destabilization series, we add the possibility to keep the form factor fixed during the calculation. This is justified for silica particles, as they do not change their shape or size during the destabilization process. The form factor with an added free amplitude factor is taken from the scattering curves measured at high dilution, where the structure factor equals one for the whole q range. For the oil emulsion samples always both form and structure factor are calculated directly from the measured data.

The computing time for the evaluation of one curve is quite high on a standard PC (1 GHz), because during the BSSA search for the correct solution thousands of structure factors have to be calculated. The computing time is 20−80 min for PY while it is several hours in the case of the HMSA. This holds for light scattering data, where no smearing effects (instrumental broadening) have to be taken into account. This would, however, be necessary for SANS and SAXS (small-angle neutron and X-ray scattering) and would lead to a further increase of computing time in those applications.

4. Results and Discussion

4.1. Sample Characterization. For the characterization of the different samples we have performed experiments at high dilution (∼0.1 vol % for silica, ∼1 vol % for emulsions). Figure 1 shows the intensity weighted size distributions calculated from the scattering curves of the different samples. For the uncoated silica, a monomodal distribution with average radius of 256 nm is found, which corresponds well with SEM images showing an average diameter of 525 nm.[33] The coated sample shows a main population which is a bit broader and the average radius (260 nm) a bit higher than the uncoated sample. But here also a second population of larger particles is found. It contains most likely some bigger aggregates originating from the coating process. The position and size of this second population is reproducible for different batches of coated silica. This second population to some extent influences our evaluation, because it has a big enough influence on the form factor to show up clearly in the pair distance distribution function.

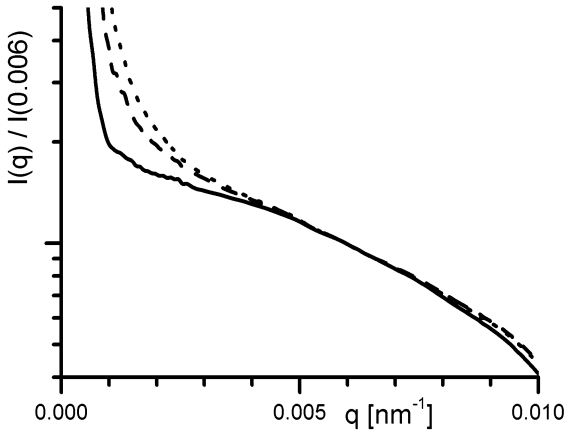

Figure 2. Scattering curves of mixtures of silica with latex at different cell thickness. For better comparability the curves have been divided by $I(0.006)$. Note that the sample measured at 98 μm is slightly different from the two others. It contains 0.085 vol % silica in a 45 wt % aqueous sucrose-solution instead of 0.1 vol % in 40 wt %, the latex content is in both cases about 0.05 vol %. Solid: 98 μm cell. Dash: 51 μm cell. Dot: 13 μm cell.

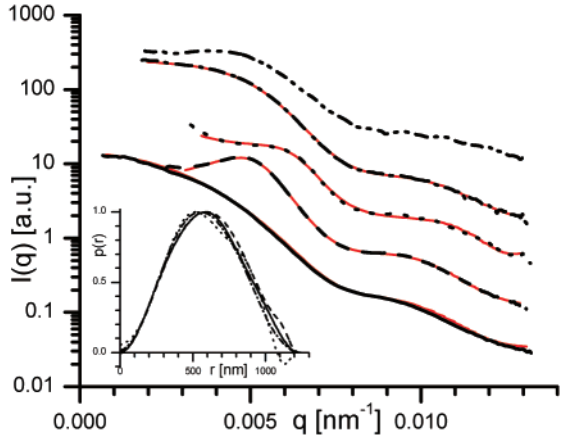

Figure 3. Scattering curves of emulsion A ($R\sim$570 nm) under different conditions; shown is the part, which can be used for evaluation. The scattering curves are shifted for better visibility. The inset shows the corresponding $p(r)$ functions. Solid: diluted. Dash: concentrated. Dot: plus Triton X100. Dash−dot: plus 26 nm latex. Dash−dot−dot: plus 76 nm latex. The fit lines from the evaluation are shown in red.

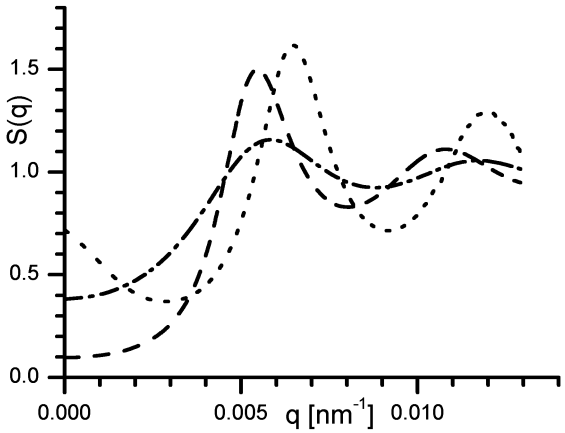

Figure 4. Structure factures for emulsion A obtained from the scattering curves in Figure 3 (same line types are used).

The two silicone oil emulsions, with average radii of 570 nm (emulsion A) and 400 nm (emulsion B), respectively, show a second population of smaller particles. But in contrast to the coated silica suspension the contribution to the scattering intensity is small and does not lead to a noticeable effect during the evaluation. All pair distance distribution functions for these samples (diluted, attractive or repulsive) correspond to those of the population of larger droplets.

4.2. Wall Effects. Most measured scattering curves of concentrated samples show a strong upturn at low q values. This happens for both repulsive and attractive systems. This upturn most likely results from a layer of particles at the glass walls of the sample-cell. If this is the case, the effect should diminish with increasing cell thickness. For this reason we measure a mixture of silica and latex at different cell thicknesses, varying from 13 to 98 μm. Figure 2 shows the obtained scattering curves. The upturn clearly shifts to lower q values with increasing cell thickness. We thus conclude that this upturn is due to wall effects.

When going to thicker cells the upturn shifts to lower q values and a wider range of the scattering curve can be evaluated. The inner part which still can be evaluated and is not affected by this upturn can be determined by a simple Guinier approximation[40] (linear in a ln I vs q^2 plot). For the measurements a compromise between avoiding the upturn at low q (thicker sample-cell) and reducing multiple scattering (thinner sample-cell) has to be found.

Another way to deal with multiple scattering would be the 3D cross-correlation technique,[41] which suppresses multiple scattering physically. But up to now this technique does not allow a time-resolved measurement.

4.3. Silicone Oil Emulsions. *4.3.1. Depletion Interaction.* The scattering curves of differently treated emulsions A ($R = 570$ nm) are depicted in Figure 3. From the diluted sample the size distribution (using ORT—see above) and the $p(r)$ function (using GIFT) are calculated for comparison. The concentrated suspension ($\phi_{oil} \sim 0.3$, 30 wt % sucrose) is measured as a representation of a repulsive hard sphere system.

The corresponding structure factors determined from these scattering curves are shown in Figure 4. The scattering curve from the concentrated sample is evaluated using the PY closure relation and a hard sphere potential. The other two structure factors are also calculated using PY, but this time with a depletion potential (eq 11). A structure factor for the scattering curve of emulsion A with 76 nm latex cannot be calculated, because the scattering from the latex particles already contributes essentially to the total scattering curve (note increase at high q values).

In Table 1, the obtained $S(q)$ parameters are compared to the ones calculated from the preparation. The sizes of the latex spheres is that stated by the manufacturer, the size of the Triton X100 micelles was taken from earlier measurements in the literature.[42] The $p(r)$ functions (inset in Figure 3) of the diluted and the concentrated sample fit together well. The ones from the attractive interacting samples show only minor differences to these two.

The scattering curves for different preparations of emulsion B are shown in Figure 5. The scattering curve of the diluted sample is mainly measured and evaluated for comparison. The $p(r)$ function is used to check if the emulsion itself changes during preparation (coalescence).

In Figure 6 the structure factors obtained from these scattering curves are depicted. The structure factor models we have used are the same as described above for emulsion A. Table 1 lists the $S(q)$ parameters obtained from the GIFT evaluation compared to those from the sample preparation. The $p(r)$ function of the sample containing latex corresponds well to the two from the diluted and concentrated emulsion (see inset in Figure 5),

TABLE 1: Comparison between $S(q)$ Parameters Obtained from GIFT Evaluation of the Scattering Curves and the Ones Calculated from the Sample Preparation[a]

	emulsion A			emulsion B		
sample	concnd	+ Triton X100	+ latex	concnd	+ Triton X100	+ latex
ϕ_{large}, preparation	0.313	0.312	0.175	0.194	0.216	0.227
ϕ_{large}, GIFT	0.297	0.343	0.163	0.209	0.221	0.224
R_{large} (nm), preparation	570	570	570	400	400	400
R_{large} (nm), GIFT	580	583	573	429	411	441
ϕ_{small}, preparation		0.029	0.034		0.067	0.036
ϕ_{small}, GIFT		0.027	0.040		0.050	0.047
$\eta_p^{(R)}$, GIFT		0.042	0.048		0.065	0.063
$2R_{small}$ (nm), preparation	-	~10	~26	-	~10	~26
$2R_{small}$ (nm), GIFT	-	12	23	-	11	24
size ratio, GIFT	-	0.010	0.020	-	0.013	0.027

[a] Note that the GIFT routine calculates $\eta_p^{(R)}$ and the size ratio, the values for comparison (ϕ_{small} and $2R_{small}$) are derived from these values.

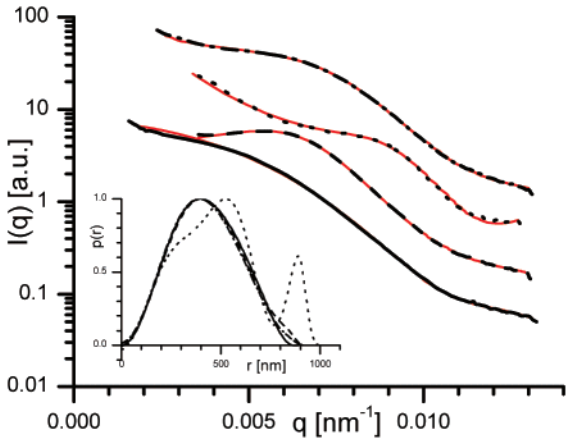

Figure 5. Scattering curves of emulsion B ($R \sim 400$ nm) under different conditions; shown is the part, which can be used for evaluation. The scattering curves are shifted for better visibility. The inset shows the corresponding $p(r)$ functions. Solid: diluted. Dash: concentrated. Dot: plus Triton X100. Dash−dot: plus 26 nm latex. The fit lines from the evaluation are shown in red.

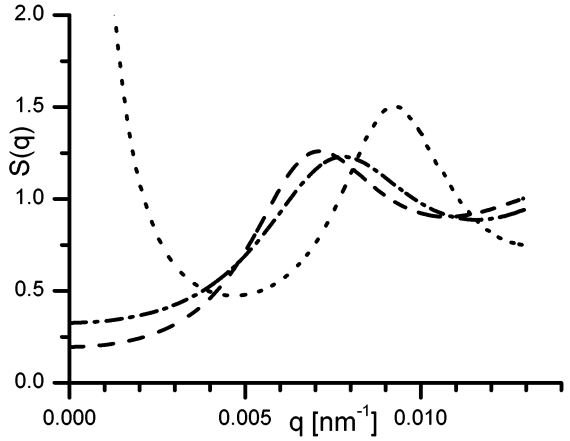

Figure 6. Structure factures of emulsion B obtained from the scattering curves in Figure 5 (same line types are used). The structure factor for the emulsion with Triton X100 reaches a value of 5 at $S(0)$.

but the $p(r)$ function for the emulsion with Triton X100 differs noticeable from the other three. One can deduce from this $p(r)$ that the emulsion has undergone some coalescence during the preparation—most likely during the addition of sucrose.

4.3.2. Comparison of Different Structure Factor Models. The above examples show that it is possible to evaluate scattering data from attractive interacting systems and get reasonable results. Now the question arises how reliable this procedure is or if wrong structure factor models lead to similar results and

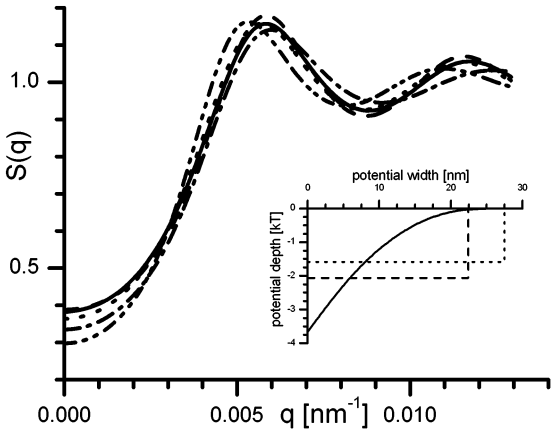

Figure 7. Structure factors calculated from the scattering curve of a mixture of emulsion A and 26 nm latex (dash−dot curve in Figure 3) using different structure factor models. The inset shows the corresponding potentials for the attractive models. Solid: PY with depletion potential. Dash: HMSA with square well Dot: PY with square well. Dash−dot: hard sphere without limits. Dash−dot−dot: hard sphere with narrow limits.

fits. Can one deduce from the fit quality and the obtained parameters if the used structure factor model is correct?

To answer this questions, we evaluate the scattering curve from emulsion A plus 26 nm latex using different structure factor models. Used are the following: depletion potential with PY, square well potential with HMSA, and square well potential with PY, as well as a repulsive hard sphere potential with PY. In the case of the false model, the hard sphere potential, we perform two different kinds of evaluation. In one case, we limit the search region for the parameters defining the structure factor (radius, volume fraction) just to physically possible values. In a second run, we keep these limits rather narrow around the values known from preparation. Figure 7 shows the structure factors obtained from these evaluations. For the depletion potential and the hard sphere potential with narrow limits the fit quality is shown in Figure 8.

As long as using an attractive potential the results are satisfactory. The depletion potential (in combination with PY) describes the actual system most accurate. Therefore, as expected, the fit to the data is best and the obtained parameters are correct. The square well potential already is a simplification. Still the results are quite satisfactory, but some information is lost. The concentration of the small particles cannot be derived from this potential, whereas the width of the square well corresponds well with their size. The depth of the square well is about half the depth of the depletion potential (see inset in Figure 7). So the actual depletion potential can be approximated by a square well potential with reasonable quality.

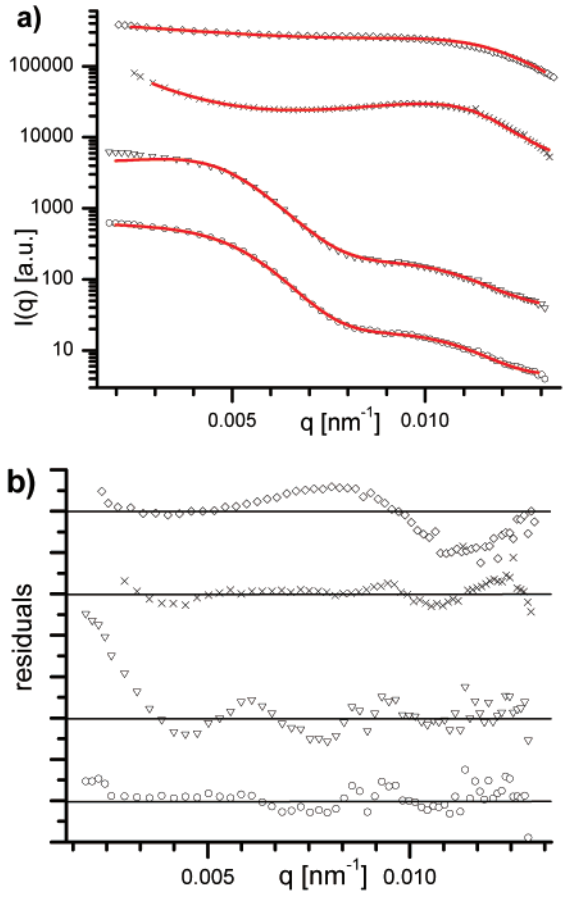

Figure 8. Comparison of the quality of different fits. Circles: emulsion A plus 26 nm latex evaluated using PY with depletion potential. Triangles: emulsion A plus 26 nm latex evaluated using PY with hard sphere potential and narrow limits for the parameters. Crosses: typical fit for ΔpH method (DCC). Diamonds: typical fit for Δ*I* method (DCC). Part a: fit lines to the measured curves in red. Part b: residual plots from nonlinear least-squares fit. The plots are shifted for better visibility but are on the same scale.

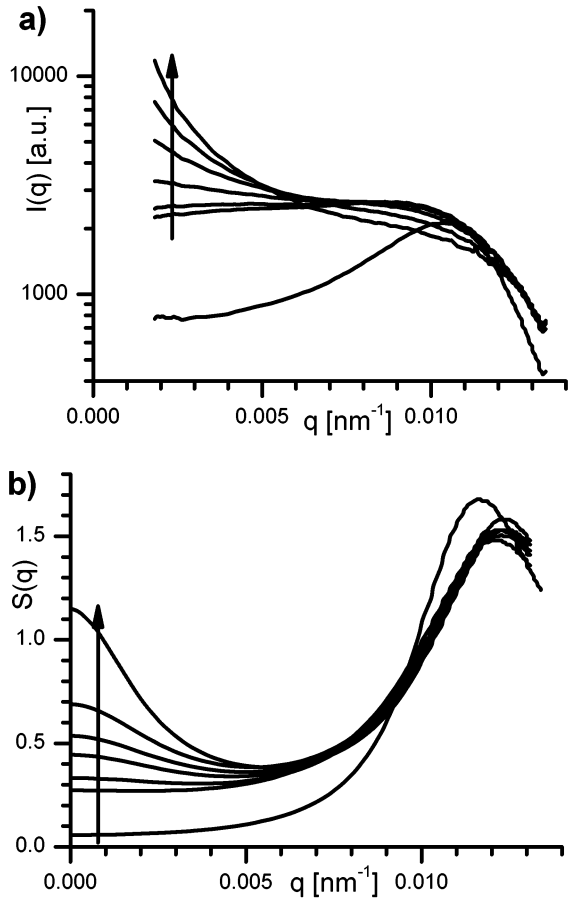

Figure 9. Part a: scattering curves from the ionic strength shift destabilization, shown is the part, which can be used for evaluation. The sequence (following the arrow) is as follows: stable suspension, 100 s, 140 s, 180 s, 220 s, 260 s, and 360 s after enzyme addition. Part b: structure factors calculated from the scattering curves using a HMSA-closure relation with a square well potential. In direction of the arrow: stable, 200 s, 220 s, 240 s, 260 s, 280 s, and 360 s after enzyme addition.

When a hard sphere model is used for data evaluation the results are different. If the $S(q)$ parameters (volume fraction and radius) are forced into a narrow band close to the actual ones the obtained solution fits to the data very badly. Without restricting the search regime for the $S(q)$ parameters the resulting fit is better, but still not very good. However, in this case the obtained parameters are quite different from the actual ones. The obtained volume fraction of the large particles is 0.13 instead of 0.175 and the radius 478 instead of 570 nm.

From the above example one can see that it is possible to recognize the use of an incorrect structure factor model (repulsive instead of attractive) by the quality of the obtained fit. The system in this example (silica with latex) is a relatively moderate attractive system. The misfit will be bigger for more attractive systems. If some a priori information about the system is available the situation is even clearer. When using a square well potential instead of the depletion potential, which are both attractive, the obtained results are still reasonable. One just loses a piece of information, the concentration of the smaller particles.

One more remark about a priori information about the system. It is not just helpful to decide if the correct structure factor model was chosen, but sometimes it is necessary. It has already been shown for charged systems[43] that different sets of parameters can lead to identical structure factors. The same is true for these attractive structure factor models. This and the quasi linear dependence of the parameters (see point 3.6) makes it necessary to limit one or two of the parameters to a rather small regime. Usually this should prove no problem. For example when studying interactions mostly the properties of the used particles, like their size or concentration, are quite well-defined and known—like in the following DCC experiments.

4.4. Silica Suspensions. *4.4.1. Depletion Interaction.* The scattering curve with 98 μm cell thickness in Figure 2 is used for the structure factor calculation. This is done to test the GIFT evaluation on another model system for depletion interaction. The $S(q)$ parameters obtained from the calculation match well to the values known from the preparation. The values obtained from the GIFT evaluation are as follows: $\phi_{\text{silica}} = 0.093$, interaction radius = 271 nm, $\phi_{\text{latex}} = 0.071$, and latex size = 22 nm. As for the silicon oil emulsion, a depletion potential in combination with PY can successfully be used to correctly evaluate this system.

4.4.2. Direct Coagulation Casting. Detailed results from these destabilizations have already been presented in another paper; for a detailed description, we refer to ref 33. Figures 9 (Δ*I* method) and 10 (ΔpH method) summarize the results from the two destabilization experiments. Shown are the scattering curves and the calculated structure factors. For comparison the scattering curves and structure factors for the corresponding stable systems are also shown.

The scattering curves at the very beginning of the destabilization cannot be evaluated, neither using a repulsive nor an

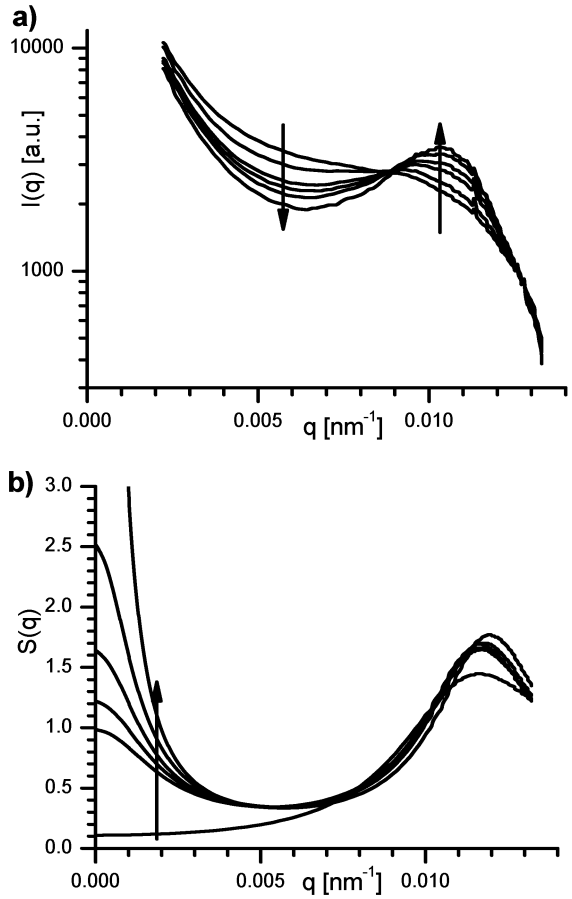

Figure 10. Part a: scattering curves from the pH shift destabilization, shown is the part, which can be used for evaluation. The sequence (following the arrows) is as follows: stable suspension, 660 s, 1260 s, 1860 s, 2700 s, and 3930 s after enzyme addition. Part b: structure factors calculated from the scattering curves using a HMSA-closure relation with a square well potential. In direction of the arrow: stable, 980 s, 1260 s, 1860 s, 2700 s, and 3930 s after enzyme addition.

attractive potential. The system seems to be in an intermediate state, where the attractive interaction just evolves. After this initial period the scattering curves can be evaluated well using a square well potential. Finally after some destabilization time the scattering curves no longer change with time, the resolution limit of our instrument is reached. We achieve $q_{min} = 0.0018$ nm^{-1} for the ΔI method and $q_{min} = 0.0021$ nm^{-1} for the ΔpH method. The suspensions are still liquid at this stage as the destabilization goes on and leads to a solid gel only at a later stage of the reaction. For the data from uncoated silica (ionic strength shift) the form factor has to be fixed for the evaluation of $S(q)$. Otherwise the program does not converge to a solution. All the calculated curves show a slight systematic misfit to the measured data in the peak-region (around $q \sim 0.011$ nm^{-1}, see Figure 8). This is a clear hint that the used simple square well potential does not reproduce the actual potential of the system appropriately. However, the obtained potential parameters are reasonable and correspond well to the potentials calculated using DLVO theory. The structure factors themselves show a clear and continuous trend with time.

The second population of larger particles present in the coated silica sample (ΔpH method) influences the form factor. However, this has no noticeable effects on the calculation of the structure factor. We get nearly identical form factors (and with it $p(r)$) for all evaluated scattering curves—diluted, repulsive, and attractive. The structure factors again show a clear trend with time as well as the corresponding parameters. The overall obtained fit (see Figure 8) is better than for the ΔI method.

For both destabilizations the parameters corresponding to the calculated structure factors fit well to those known from the preparation or obtained from DLVO calculations. Volume fraction and interaction radius are always a little bit larger than the actual silica content and size. This can be attributed to the fact that our simple square well model does not take charges into account. The parameters defining the potential fit, within the given experimental accuracy, well to potentials calculated using DLVO theory.

5. Discussion and Conclusion

We are able to evaluate light scattering curves of various attractively interacting samples using the generalized indirect Fourier transformation. In the case of the direct coagulation casting samples, we can follow the potential change in the system in real time. For the evaluation we can choose between different structure factor models—PY or SMSA depletion potential and PY, HMSA, or SMSA square well potential. All final results give a good fit to the measured data and yield reasonable parameters defining the structure factor. Taking into account the approximations that have to be made, the quality of the results is quite good.

To get a reasonable solution within acceptable time one should possess some a priori information about the investigated system. Because of the dependence of the four $S(q)$ parameters, which has already been described above, this information is needed to confine one or two parameters. With this restriction the GIFT method usually leads to a correct solution. As can be seen for the ΔI destabilization samples, the available potentials (depletion and square well) are not always sufficient to render the actual potentials. Nevertheless, they give an acceptable approximation.

In an attractively interacting sample, there is always the possibility of cluster formation, which would contribute to the scattering curve al low q. Cluster formation and attractive interaction appear together and change the scattering curve similarly. But as long as the attractive potential is not too strong, the clusters still can break up and their contribution to the scattering curve should be negligible. For weak attractive potentials $U_{attr} \geq k_B T$ the bonds between the particles are weak enough that aggregation and thermal rearrangement compete.[44,45] There still is an actual probability that particles can get away again from an already formed cluster. The deepest (calculated) potential of all our samples was $-5kT$ for emulsion plus Triton X100. This sample macroscopically already shows an increased viscosity.

The structure factor routines themselves are also limited to a certain potential depth. The square well potential is limited to a well depth between $-2kT$ and $-3kT$ depending on the width of the potential. The depletion potential can reach a maximum depth around $-6kT$. The necessary computing time is directly related to the strength of the attractive potential. The more attractive, the longer the computing time needed.

Beside the light scattering data presented in this study some preliminary calculations on SANS data from attractively interacting systems have also been performed. The first results look promising, and it will be surely possible to apply the presented technique to other systems.

Acknowledgment. We acknowledge fruitful discussions with Rudolf Klein and Johan Bergenholtz and thank Johan Bergenholtz for providing the structure factor routines. We acknowl-

edge financial support by the Austrian Science Foundation (FWF) under Project P15698 and support by the Marie Curie Network MRTN-CT-2003-504712.

References and Notes

(1) Evans, D. F.; Wennerström, H. *The Colloidal Domain*; VCH: New York, 1994.
(2) Hiemenz, P. C.; Rajagopalan, R. *Principles of Colloids Surface Chemistry*, 3rd ed.; Marcel Dekker: New York, 1997.
(3) Hunter, R. J. *Foundations of Colloid Science*, 2nd ed.; Oxford Universiy Press: New York, 2001.
(4) Meyers, D. *Surfaces, Interfaces, and Colloids*, 2nd ed.; Wiley-VCH: New York, 1999.
(5) Dawson, K. A. *Curr. Opin. Colloid Interface Sci.* **2002**, *7*, 218.
(6) Prasad, V.; Trappe, V.; Dinsmore, A. D.; Segre, P. N.; Cipelletti, L.; Weitz, D. A. *Faraday Discuss.* **2003**, *123*, 1.
(7) Fu, D.; Lie, Y.; Wu, J. *Phys. Rev. E* **2003**, *68*, 011403/1.
(8) Feng, J.; Ruckenstein, E. *J. Colloid Interface Sci.* **2004**, *272*, 430.
(9) Sandkuehler, P.; Sefcik, J.; Morbidelli, M. *Adv. Colloid Interface Sci.* **2004**, *108*−*109*, 133.
(10) Lindner, P.; Zemb, T. *Neutrons, X-rays and Light: Scattering Methods Applied to Soft Condensed Matter*; Elsevier Science: Amsterdam, 2002.
(11) Lorenz, L. *Videnskab. Selskab. Skrifter*. **1890**, *6*, 1.
(12) Mie, G. *Ann. Phys.* **1908**, *25*, 377.
(13) Rayleigh, D. W. *Proc. R. Soc. A* **1914**, *90*, 219.
(14) Debye, P. *Ann. Phys.* **1915**, *46*, 809.
(15) Gans, R. *Ann. Phys.* **1925**, *76*, 29.
(16) Klein, R.; D'Aguanno, B. Static scattering properties of colloidal suspensions. In *Light Scattering: Principles and Development*; Brown, W., Ed.; Claredon Press: Oxford, England, 1996; p 30.
(17) Weyerich, B.; Brunner-Popela, J.; Glatter, O. *J. Appl. Crystallogr.* **1999**, *32*, 197.
(18) Brunner-Popela, J.; Glatter, O. *J. Appl. Crystallogr.* **1997**, *30*, 431.
(19) Glatter, O. *J. Appl. Crystallogr.* **1977**, *10*, 415.
(20) Percus, J. K.; Yevick, G. J. *Phys. Rev.* **1958**, *110*, 1.
(21) Rogers, F. J.; Young, D. A. *Phys. Rev. A* **1984**, *30*, 999.
(22) Zerah, G.; Hansen, J. P. *J. Chem. Phys.* **1986**, *84*, 2336.
(23) Bergmann, A.; Fritz, G.; Glatter, O. *J. Appl. Crystallogr.* **2000**, *33*, 1212.
(24) Lindner, H.; Fritz, G.; Glatter, O. *J. Colloid Interface Sci.* **2001**, *242*, 239.
(25) Asakura, S.; Oosawa, F. *J. Chem. Phys.* **1954**, *22*, 1255.
(26) Asakura, S.; Oosawa, F. *J. Polym. Sci.* **1958**, *33*, 183.
(27) Vrij, A. *Pure Appl. Chem.* **1976**, *48*, 471.
(28) Ilett, S. M.; Orrock, A.; Poon, W. C. K.; Pusey, P. N. *Phys. Rev. E* **1995**, *51*, 1344.
(29) Lekkerkerker, H. N. W.; Poon, W. C. K.; Pusey, P. N.; Stroobants, A.; Warren, P. B. *Europhys. Lett.* **1992**, *20*, 559.
(30) Bergenholtz, J.; Poon, W. C. K.; Fuchs, M. *Langmuir* **2003**, *19*, 4493.
(31) Mabille, C.; Schmitt, V.; Gorria, P.; Calderon, F. L.; Faye, V.; Deminière, B.; Bibette, J. *Langmuir* **2000**, *16*, 422.
(32) Bibette, J. *J. Colloid Interface Sci.* **1991**, *147*, 474.
(33) Wyss, H. M.; Innerlohinger, J.; Meier, L. P.; Gaukler, L. J.; Glatter, O. *J. Colloid Interface Sci.* **2004**, *271*, 388.
(34) Gauckler, L. J.; Graule, T.; Baader, F. *Mater. Chem. Phys.* **1999**, *61*, 78.
(35) Gauckler, L. J.; Graule, T.; Baader, F.; Will, J. *Key Eng. Mater.* **1999**, *159*−*160*, 135.
(36) Lehner, D.; Kellner, G.; Schnablegger, H.; Glatter, O. *J. Colloid Interface Sci.* **1998**, *201*, 34.
(37) Schnablegger, H.; Glatter, O. *Appl. Opt.* **1991**, *30*, 4889.
(38) Bergenholtz, J.; Wagner, N. J.; D'Aguanno, B. *Phys. Rev. E* **1996**, *53*, 2968.
(39) Bergenholtz, J.; Wu, P.; Wagner, N. J.; D'Aguanno, B. *Mol. Phys.* **1996**, *87*, 331.
(40) Guinier, A. *Ann. Phys.* **1939**, *12*, 161.
(41) Urban, C.; Schurtenberger, P. *J. Colloid Interface Sci.* **1998**, *207*, 150.
(42) Stubicar, N.; Matejas, J.; Zipper, P.; Wilfing, R. Size, shape and internal structure of Triton X-100 micelles determined by light and small-angle X-ray scattering techniques. In *Surfactants in Solution*, Mittal, K. L., Ed.; Plenum Publishing Corporation: New York, 1989; Vol. 7, p 181.
(43) Fritz, G.; Bergmann, A.; Glatter, O. *J. Chem. Phys.* **2000**, *113*, 9733.
(44) Poon, W. C. K.; Haw, M. D. *Adv. Colloid Interface Sci.* **1997**, *73*, 71.
(45) Haw, M. D.; Sievwright, M.; Poon, W. C. K.; Pusey, P. N. *Adv. Colloid Interface Sci.* **1995**, *62*, 1.